pH-Responsive Poly(D,L-lactic-*co*-glycolic acid) Nanoparticles with Rapid Antigen Release Behavior Promote Immune Response

Qi Liu,[†,‡] Xiaoming Chen,[†,‡] Jilei Jia,[†,‡] Weifeng Zhang,[†,‡] Tingyuan Yang,[†] Lianyan Wang,[*,†] and Guanghui Ma[*,†,§]

[†]National Key Laboratory of Biochemical Engineering, PLA Key Laboratory of Biopharmaceutical Production & Formulation Engineering, Institute of Process Engineering, Chinese Academy of Sciences, Beijing, 100190, People's Republic of China, [‡]University of Chinese Academy of Sciences, Beijing, 100049, People's Republic of China, and [§]Collaborative Innovation Center of Chemical Science and Engineering (Tianjin), Tianjin, 300072, People's Republic of China

ABSTRACT In the quest to treat intracellular infectious diseases and virus infection, nanoparticles (NPs) have been considered to be efficient tools for inducing potent immune responses, specifically cellular immunity. Antigen processing and presenting by antigen presenting cells (APCs) could influence immune response, especially the priming of T-cell-mediated cellular immunity. Here, we fabricated pH-responsive poly(D,L-lactic-*co*-glycolic acid) (PLGA) NPs with rapid antigen intracellular release behavior in APCs. The NPs, which had thin shells and large inner space, contain ammonium bicarbonate (NH_4HCO_3), which could regulate release in endosomes and lysosomes, acting as an antigen release promoter in dendritic cells (DCs), and were coencapsulated with antigen (ovalbumin, OVA). Hydrogen ions (H^+) in DC endosomes and lysosomes (pH ~5.0 and 6.5) could react with NH_4HCO_3 to generate NH_3 and CO_2, which broke NPs and released antigens. After uptake by DCs, antigens encapsulated in pH-responsive PLGA NPs could escape from lysosomes into the cytoplasm and be cross-presented. Moreover, the NPs induced up-regulation of co-stimulatory molecules and stimulated cytokine production. Mouse immunization with pH-responsive PLGA NPs induced greater lymphocyte activation, more antigen-specific $CD8^+$ T cells, stronger cytotoxic capacity (IFN-γ and granzyme B), enhanced antigen-specific IgG antibodies, and higher serum IgG2a/IgG1, indicating cellular immunity. The NPs also improved generation of memory T cells to protect against reinfection. Thus, pH-responsive PLGA NPs, which induced strong cellular immune responses and offered antibody protection, could be potentially useful as effective vaccine delivery and adjuvant systems for the therapy of intracellular infectious diseases and virus infection.

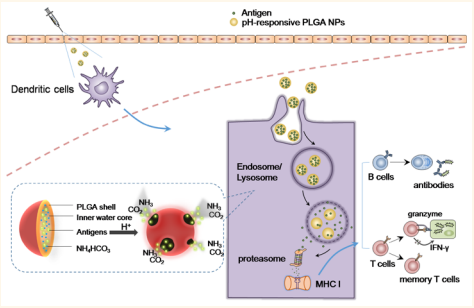

KEYWORDS: antigen intracellular rapid release · dendritic cells · pH-responsive · PLGA nanoparticles · vaccine delivery and adjuvant system

Intracellular infectious diseases and virus infection have contributed to worldwide morbidity and mortality, and such a global burden induced by pathogens such as HBV, tuberculosis, and HIV emphasizes the urgent need for new and effective vaccinations and infection treatment strategies.[1] Vaccination is one of the oldest and still most useful methods for generating humoral and cellular immune responses to prevent infectious diseases. Recent findings have indicated that T cell immunity is key to limiting disease severity, and induction of antigen-specific T-cell-mediated cellular immune responses is the ultimate goal of vaccination, requiring specific antigens and appropriate adjuvants. Although aluminum salts such as aluminum hydroxide or phosphate have been used for many antigens, they are not suitable for all antigens and have disadvantages of side effects and safety concerns.[2,3] Moreover, aluminum-based vaccines, which function as an "antigen depot" for retaining antigen at the injection site, are thought to induce poor activation and maturation of APCs and offer only weak T-cell-mediated immune responses, which are indispensable for killing intracellular pathogens.[4−7] To overcome these limitations, new biocompatible particulate antigen-delivery systems are being developed.[8] Nanoparticle (NP)-based

* Address correspondence to wanglianyan@home.ipe.ac.cn (L.-Y. Wang), ghma@home.ipe.ac.cn (G.-H. Ma).

Received for review November 23, 2014 and accepted April 21, 2015.

Published online April 21, 2015
10.1021/nn5066793

vaccine formulations are available in diverse sizes and comprise various materials. The materials that have been investigated in the past included polysaccharide (*e.g.*, starch, alginate, agarose), proteins (*e.g.*, gelatin, albumin), fats and fatty acids (*e.g.*, palmitic acid), lipids, and polymers. Each of these materials could offer their own advantages, and to date, a series of NPs, such as poly(lactic acid) (PLA), poly(D,L-lactic-*co*-glycolic acid) (PLGA), and chitosan (CS), have been applied as adjuvants to enhance vaccine efficiency.[9−11] However, PLGA, an FDA-approved synthetic biodegradable polymer, has gained a lot of attention and has also been used for NP formation and extensively applied in vaccine delivery. While, cellular immunity was still limited since surface modification was necessary for NPs to enhance adjuvant effects.[12−15]

Induction of immune response involves several steps that feature antigen presenting cells (APCs), which take up and process antigens, prime T cells, and activate B cells. Dendritic cells (DCs), the most potent and crucial APCs, are essential for initiating and regulating vaccine-induced immune responses.[16,17] Upon immunization, DCs capture antigens and migrate into lymph nodes and spleen, where they present the digested antigen peptides to $CD4^+$ and $CD8^+$ T cells and then trigger adaptive cellular immune responses with the help of co-stimulatory molecules.[18] Moreover, DCs release numerous cytokines upon activation, regulating both innate and adaptive immunity.[19] DCs also participate in antibody generation through their interactions with B cells.[20] With such a pivotal role of DCs in vaccine-induced immune responses, researchers focused on designing particulate antigen-delivery systems based on DCs. Recent studies have indicated that the intracellular environment where interactions between antigens and DCs occurred could deliver signals instructing them to generate the appropriate immune responses.[21] Effective vaccination to kill intracellular pathogens often requires $CD8^+$ cytotoxic T cell responses, which only occur when antigens are processed *via* cross-presentation after uptake by DCs.[22] Particle physicochemical characteristics dictate whether they will be suitable for antigen delivery, and how NPs release antigens intracellularly to modulate the immune response is uncertain.

To address this question, we developed pH-responsive PLGA NPs for rapid antigen release based on different intracellular pH values of DCs and compared the induced immune response with normal PLGA NPs (slow release of antigens). PLGA NPs with narrow size distribution were prepared by both a facile method combining W/O/W emulsion−diffusion−extraction approach and the premix membrane emulsification technique. We adjusted the structure of normal PLGA NPs to have thinner shells and a larger inner space, while coencapsulating NH_4HCO_3 as an antigen release promoter to interact with protons in DC endosomes/lysosomes (pH ~5.0 and 6.5). Production of CO_2 and NH_3 disrupted the NP shell wall, causing antigen release. Very recently, Ruff *et al*. described the synthesis of antigen-loaded, pH-sensitive polymethacrylamide hydrogel NPs. These agents utilized an acid-sensitive cross-linker, which was copolymerized with acrylamide by inverse emulsion polymerization. The NPs thus produced were taken up and presented by bone-marrow-derived dendritic cells (BMDCs) *in vitro* and DCs and monocytes *in vivo*.[23] Unlike their work, PLGA and NH_4HCO_3 were used in our methodology, where PLGA was the FDA-approved synthetic biodegradable polymer and NH_4HCO_3, a simple and more commercially amenable agent, was used as an antigen release promoter. Combined with adjusting the ratio of the inner water phase and oil phase, we succeeded in endowing biodegradable PLGA NPs with intracellular rapid antigen release behavior for vaccine adjuvants in this paper. Here, pH-responsive and normal PLGA NPs were used to investigate whether and how antigen release within DCs affected antigen processing, presentation, and subsequent immune response, specifically T-cell-mediated responses.

RESULTS AND DISCUSSION

Characteristics of pH-Responsive PLGA NP-Based Vaccine Adjuvants. Using the W/O/W emulsion−diffusion−extraction method combined with the premixed membrane emulsification technique, we successfully fabricated uniform-sized pH-responsive PLGA NPs with rapid antigen release behavior by adjusting the ratio of the inner water phase and oil phase and adding NH_4HCO_3 (2.5 mg/mL) in the inner water phase. For PLGA polymers, a lactic/glycolic molar ratio of 75:25 was chosen. NPs prepared from copolymers with high lactic acid concentration degrade slower than those with a high glycolic acid content. Uniform-sized normal PLGA NPs without the designed structure or antigen release promoter were also prepared using the W/O/W emulsion−diffusion−extraction method combined with the premixed membrane emulsification technique. Both normal and pH-responsive PLGA NPs were of similar size, size distributions, surface zeta potential, and antigen loading efficiency (Table 1). Compared to normal PLGA NPs, pH-responsive NPs designed in this study had thinner shells and larger cavities, as shown with scanning electron microscopy (SEM) and transmission electron microscopy (TEM) images (Figure 1A, B). X-ray diffraction (XRD) patterns (Figure 1C) revealed that NH_4HCO_3 as an antigen release promoter was successfully entrapped within the NPs, and loaded antigen activity was retained from the analysis results of fluorescent and CD spectra (Supporting Information, Figure S1). Both pH-responsive PLGA NPs and normal PLGA NPs were nonporous from the analysis results of adsorption−desorption isotherms

TABLE 1. Characteristics of PLGA NP-Based Vaccine Adjuvants (Means ± SEM)

particles	diameter (nm)	PDI[a]	zeta potential[b] (mV)	antigen content (μg/mg)
pH-responsive PLGA NPs	893.63 ± 7.93	0.061 ± 0.01	−12.22 ± 2.37	49.22 ± 2.58
normal PLGA NPs	909.23 ± 4.51	0.088 ± 0.02	−17.74 ± 3.88	50.45 ± 2.17

[a] PDI, polydispersity index from dynamic light scattering (DLS). [b] Zeta potential of different NPs was detected in ultrapure water.

and Brunauer−Emmett−Teller (BET) specific surface area (Supporting Information, Figure S2). Antigen release behaviors from NPs under different pH values (7.4, 6.5, and 5.0) were studied to evaluate antigen intracellular release behavior in the endosome/lysosome and cytoplasm environment of DCs. Normal PLGA NPs offered controlled release at the same pHs within 24 h, and cumulative release efficiency was less than 10% (Figure 1E). However, pH-responsive NPs had pH-dependent antigen release (minimal at pH 7.4 and 10% within 24 h; more than 85% antigen release at pH 5.0 and 6.5 for 24 h; Figure 1D). SEM images were used to exhibit the morphological changes in pH-responsive PLGA NPs and normal PLGA NPs during antigen release incubated in media with different pH values mimicking the intracellular environment of DCs (Supporting Information, Figure S3). Antigen release was depicted in Figure 1H. In acidic environments, the proton infiltrated the PLGA shell and reacted with NH_4HCO_3 to produce gas bubbles, and the thinner pH-responsive NP shell was disrupted to release encapsulated antigens. To test whether the mechanism worked, we added the indicated amounts of proton scavenger during the release of antigen encapsulated by pH-responsive PLGA NPs in the acidic environment. The NPs were immersed in the acidic environment mimicking the DC intracellular endosome/lysosome (pH 6.5 and 5.0), respectively. Addition of indicated amounts of proton scavenger took place after 1, 2, and 8 h since these time points were thought to be the early, middle, and late stage during antigen release (Figure 1D). The results showed antigen release encountered different degrees of influence after addition of proton scavenger at the early (1 h), middle (2 h), and late stage (8 h) of the release period. In the environment of pH 5.0 (Figure 1F), after addition at 1 h, antigen release stagnated and maintained a relatively low cumulative release efficiency, which indicated that antigen release depended on the reaction between NH_4HCO_3 contained in the inner space of NPs and proton in the environment. The antigen release got blocked by the added proton scavenger at the early stage. After addition of proton scavenger at 2 h, the following release continued to increase at a relatively slow rate until reaching a plateau at 12 h. After addition of proton scavenger at 8 h, antigen release was hardly affected by the proton scavenger. At the middle and late stage of antigen release, the proton infiltrated the PLGA shell and reacted with NH_4HCO_3 to produce gas bubbles; then, the thinner pH-responsive NP shell was disrupted to release encapsulated antigens. Thus, antigen release was less affected by proton scavenger at the middle stage. At the late stage, the addition scarcely altered the antigen release. In the environment of pH 6.5, the same release behavior occurred when indicated amounts of proton scavenger were added at 1, 2, and 8 h (Figure 1G). These experiments determined the significance of NH_4HCO_3 contained in the inner space of NPs for regulating antigen release behavior. Whether and how antigen intracellular release affected antigen presentation, DC activation and maturation, and *in vivo* immune response were further investigated in subsequent studies.

pH-Responsive PLGA NPs Promoted Antigen Cross-Presentation *in Vitro*. DCs, the most potent APCs, were necessary for inducing protective immunity. After uptake by DCs, the intracellular fate of antigens (including intracellular localization and presentation) dramatically influenced the magnitude and quality of the immune response.[21] First, the biocompatibility of pH-responsive NPs confirmed in BMDCs *in vitro* with CCK-8 assays indicated excellent biocompatibility (Supporting Information, Figure S4). NPs could also deliver antigen to BMDCs, and pH-responsive NPs slightly promoted antigen uptake compared with normal PLGA NPs (Supporting Information, Figure S5). This was probably due to the slightly increased zeta potential of pH-responsive PLGA NPs (Table 1), which could facilitate interactions between the NPs and the negatively charged cell membrane.[24,25] After antigen uptake, intracellular trafficking of internalized NPs was measured *via* localization of antigens in NPs (labeled with FITC-OVA in green) and lysosomes, the key intracellular organelles during antigen processing and presentation (labeled with Lyso-Tracker in red). (OVA = ovalbumin; FITC = fluorescein isothiocyanate.) Efficient exogenous antigen endosomal escape was important for antigens to be presented through the MHC I pathway to activate $CD8^+$ T cells and elicit a robust CTL response.[26] Confocal images revealed that normal PLGA NPs taken up by DCs mostly colocalized with lysosomes, whereas most of antigens from pH-responsive NPs existed in the cytoplasm, indicating lysosome escape and the ability to induce a strong cytotoxic T lymphocyte (CTL) immune response (Figure 2A). As shown in Figure 2A, when BMDCs were pretreated with chloroquine, which could be used as an inhibitor of endosomal acidification, the confocal images revealed that antigens from

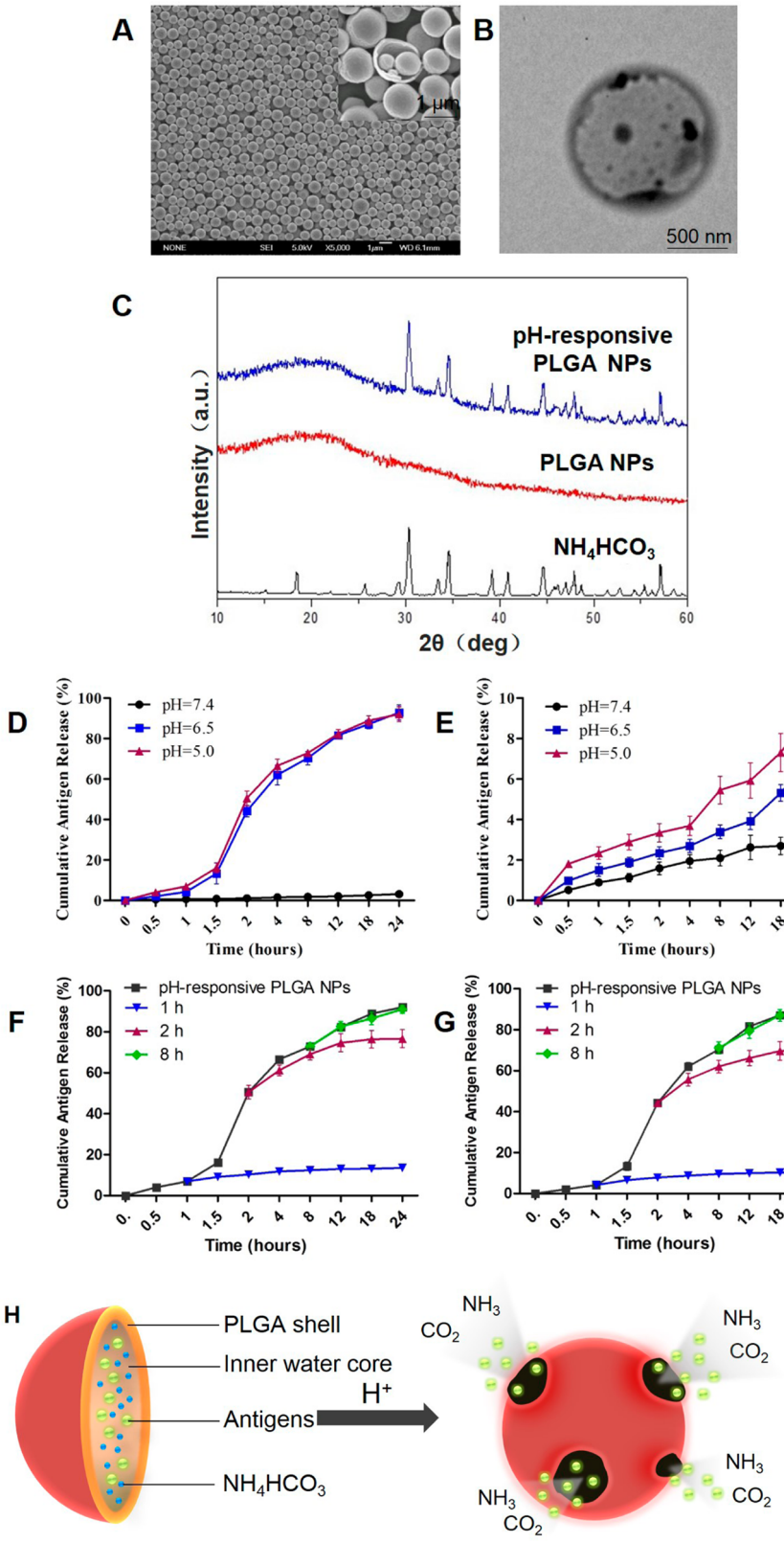

Figure 1. Characteristics of pH-responsive PLGA NP-based vaccine adjuvants: (A) SEM and (B) TEM micrographs of pH-responsive PLGA NPs; (C) XRD patterns of NH_4HCO_3, empty PLGA NPs, and pH-responsive PLGA NPs; *in vitro* release of antigens from (D) pH-responsive PLGA NPs and (E) normal PLGA NPs incubated in test media with different pH values to mimic the cytoplasm (pH 7.4), early endosomes (pH 6.5), and late endosomes/lysosomes (pH 5.0) at 37 °C. *In vitro* release of antigens from pH-responsive PLGA NPs after addition of indicated amounts of proton scavenger at 1, 2, and 8 h in the acidic environment of (F) pH 5.0 and (G) pH 6.5 at 37 °C. Data were expressed as means ± SEM ($n = 6$). (H) Schematic illustrating the composition/structure of the as-constructed pH-responsive PLGA NPs and their working mechanism.

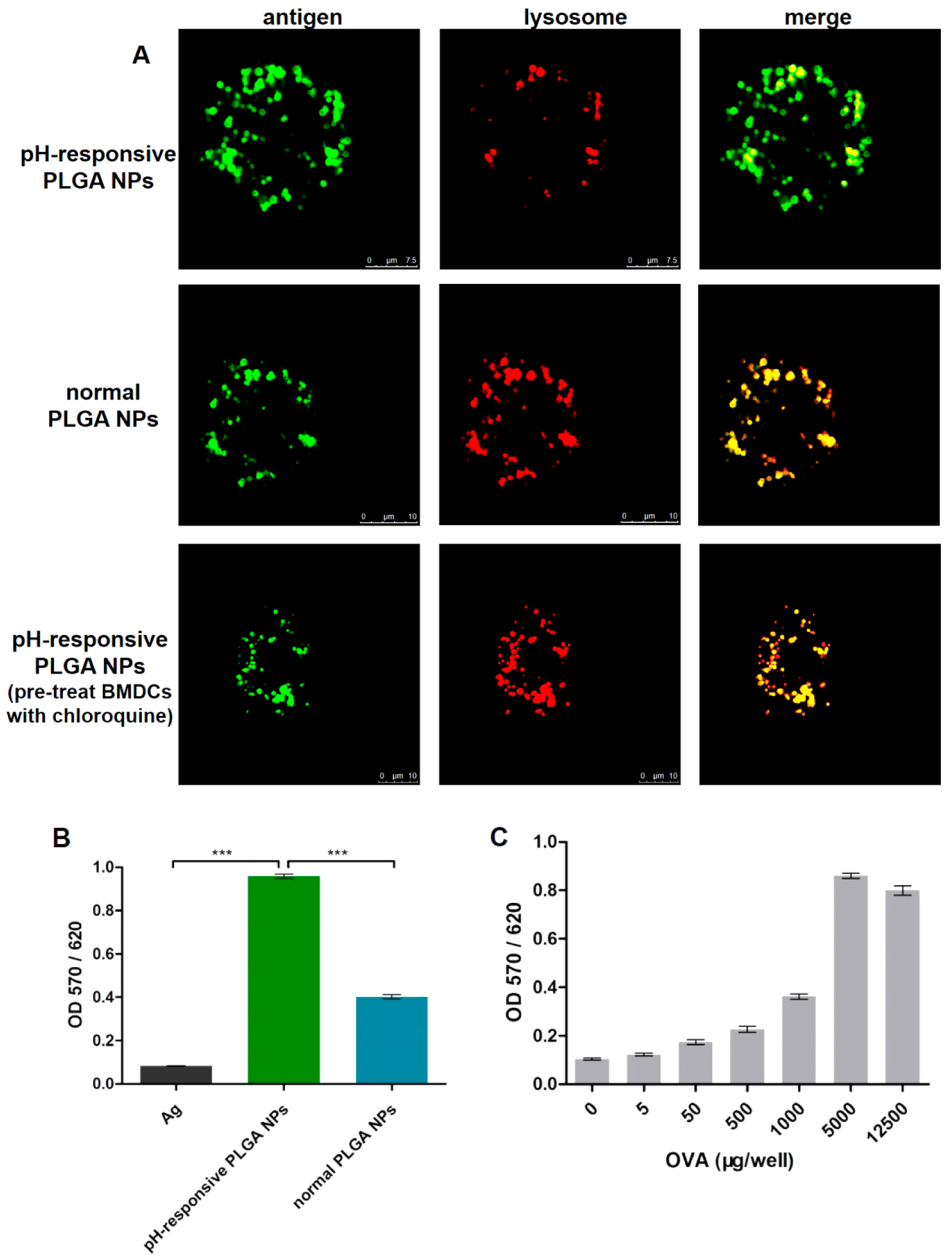

Figure 2. (A) Antigen intracellular localization from pH-responsive PLGA NPs in BMDCs, normal PLGA NPs in BMDCs, and pH-responsive PLGA NPs in BMDCs pretreated with chloroquine was observed by CLSM. Antigens were labeled by FITC (green points); lysosomes were labeled by Lyso-Tracker Red (red points). (B) Different groups of vaccine adjuvant-based OVA and (C) indicated concentrations of OVA were cross-presented by DCs and B3Z *in vitro*. Cross-presentation of B3Z cells was determined by β-galactosidase activity using a colorimetric LacZ assay (absorbance 570/620 nm). Graphs shown represent results of three independent coculture experiments. Data are expressed as means $\pm$ SEM ($n = 6$) (*$p < 0.05$; **$p < 0.01$; ***$p < 0.001$).

pH-responsive PLGA NPs mostly colocalized with the lysosome. This indicated that antigen intracellular release of pH-responsive PLGA NPs needed to be in an acidic environment. Without the interaction between the pH-responsive PLGA NPs and the proton, the NPs lost the rapid antigen release behavior and acted the same as normal PLGA NPs.

After confirming that pH-responsive NPs could efficiently be captured by DCs and escape from the lysosome into the cytoplasm, we analyzed their capacity to cross-present NP-encapsulated antigens in a B3Z cell line. B3Z, a SIINFEKL-specific $CD8^+$ T cell hybridoma line, could be activated by SIINFEKL, which was the final peptide of NP-based antigens cross-presented by DCs.[27] Cross-presentation could be evaluated by measuring activation of B3Z with a LacZ method. After coculturing DCs and B3Z with titrated amounts of NPs-OVA (1 μg/well), data indicated that pH-responsive NPs significantly enhanced cross-presentation of OVA (Figure 2B). Specifically, pH-responsive NPs cross-presented OVA 230% and 1100% of that cross-presented by normal NP-antigen

and antigen alone ($p < 0.001$). These results fully demonstrated that rapid antigen release within DCs greatly promoted antigen escape to the cytoplasm and enhanced cross-presentation.

To ensure NPs promote antigen cross-presentation, we compared cross-presentation of different concentrations of soluble OVA (Figure 2C). Notably, higher concentrations of soluble OVA were required to achieve a similar response with pH-responsive NP-encapsulated OVA. More than 1000 times soluble OVA was required to stimulate the same response observed with 1 μg/well NPs-OVA. Thus, uptake of antigen-loaded NPs and rapid antigen release behavior were essential for antigen cross-presentation, and we concluded that antigen intracellular rapid release by pH-responsive PLGA NP-based vaccine adjuvants offered efficient endosomal escape and superior cross-presentation for priming CTL killing.

pH-Responsive PLGA NPs Promoted DC Activation and Maturation *in Vitro*. After antigen processing and presentation, BMDCs expressed activation markers to prime T cells, thereby inducing antigen-specific immune responses. These results showed that the expression of CD86 and CD40 co-stimulatory markers was significantly up-regulated in the presence of pH-responsive PLGA NPs ($p < 0.05$; for CD40, compared to antigen alone, $p < 0.01$; Figure 3A,B).

Next, we tested whether activation also promoted cytokine secretion during DC maturation. pH-responsive PLGA NPs indeed induced greater production of pro-inflammatory cytokines IL-1β and IL-6 than other groups (Figure 3C,D). Secretion of Th1-polarizing cytokines IL-12p70 and TNF-α followed the trends of pH-responsive NPs that had an enhanced effect on maturation. pH-responsive NPs significantly increased production of IL-12p70 and TNF-α (Figure 3E,F). Production of typical Th-1 cytokine IL-12p70 and pro-inflammatory cytokine IL-6 were both time-dependent, especially for pH-responsive NPs (Figure 3G,H). Such a sustained enhancement of cytokine production was observed during the first few hours and plateaued at 12−24 h, which reflected rapid antigen release within DCs. This immune response could provoke the activation of $CD8^+$ T cells and potentiate cytotoxic killing of $CD8^+$ T cells.[28]

pH-Responsive PLGA NPs Promoted Lymphocyte Activation and T-Cell-Mediated Immune Response in Mice. To confirm pH-responsive PLGA NP-based vaccine adjuvanticity with regard to cellular immunity, we immunized mice with pH-responsive NPs, normal NPs, and antigen alone and evaluated lymphocyte activation, antigen-specific $CD8^+$ T cell responses, and memory T cell responses in mouse splenocytes restimulated *ex vivo*.

CD69, an activation marker, was used to measure activation of effector immune cells. B cells, $CD4^+$ T cells, and $CD8^+$ T cells of splenocytes from each test group were labeled with specific FACS antibodies. pH-responsive NPs significantly enhanced the activation of T cells more than antigen alone (for $CD4^+$ T cells, $p < 0.01$; for $CD8^+$T cells, $p < 0.001$) (Figure 4A−C; Supporting Information, Figure S6). Also, activation of B cells and $CD8^+$ T cells was both significantly improved with pH-responsive NPs more than with normal PLGA NPs ($p < 0.01$) (Figure 4A−C; Supporting Information, Figure S6). The effective activation of effector immune cells by pH-responsive PLGA NP-based vaccine adjuvants was necessary because activation of effector immune cells initiated the whole immune response.

Next, we assessed antigen-specific $CD8^+$ T cell response, which was a prerequisite of cellular immunity, using SIINFEKL-MHC I (H-$2K^b$) pentamer staining in immunized mouse splenocytes after restimulation. The frequency of antigen-specific $CD8^+$ T cells in mice immunized with pH-responsive NPs was the greatest among other groups ($p < 0.001$) (Figure 5A; Supporting Information, Figure S7). Only limited accumulation of antigen-specific $CD8^+$ T cells was observed with normal PLGA NPs and antigen alone, suggesting potential differences in effector T cell proliferation, which depended on immunization with NPs with different antigen release behaviors.

T cell response to intracellular pathogens could be characterized by differentiation of $CD8^+$ T cells into CTLs, which killed infected cells *via* granzyme secretion and differentiation of $CD4^+$ Th0 cells into $CD4^+$ Th1 cells, which secrete cytokines such as IFN-γ.[29,30] pH-responsive PLGA NPs significantly augmented the expression of granzymes and secretion of IFN-γ compared to other treatments ($p < 0.001$; for IFN-γ, compared to normal NPs, $p < 0.05$) (Figure 5B,C).

The ultimate goal of vaccination is to generate immune memory that can rapidly respond to pathogens upon reinfection, and memory T cells are important components of these memory immune responses.[31] $CD44^{hi}CD62L^{low}$ and $CD44^{hi}CD62L^{hi}$ are regarded as markers for effector-memory T cells (T_{EM}) and central-memory T cells (T_{CM}), respectively. FACS data suggested that pH-responsive NPs generated significantly more T_{EM} of $CD4^+$ T cells than normal NPs ($p < 0.05$) and antigen alone ($p < 0.01$) and remarkably more T_{EM} of $CD8^+$ T cells than normal NPs ($p < 0.05$) and antigen alone ($p < 0.01$) (Figure 6B,C). T_{CM} production was similar to T_{EM}, and pH-responsive PLGA NPs offered advantages over antigen alone and normal NPs (Figure 6A). In summary, pH-responsive PLGA NPs induced the strongest memory T cell responses, which might provide excellent protection against reinfection.

pH-Responsive PLGA NPs Promoted Production of Antigen-Specific Antibodies in Mice. To investigate whether antigen release affected humoral immunity, we assessed total antigen-specific IgG, which is indispensable for screening experimental immunological efficacy. Female C57BL/6 mice were vaccinated with 25 μg of OVA (im) with or without NPs three times at 14-day

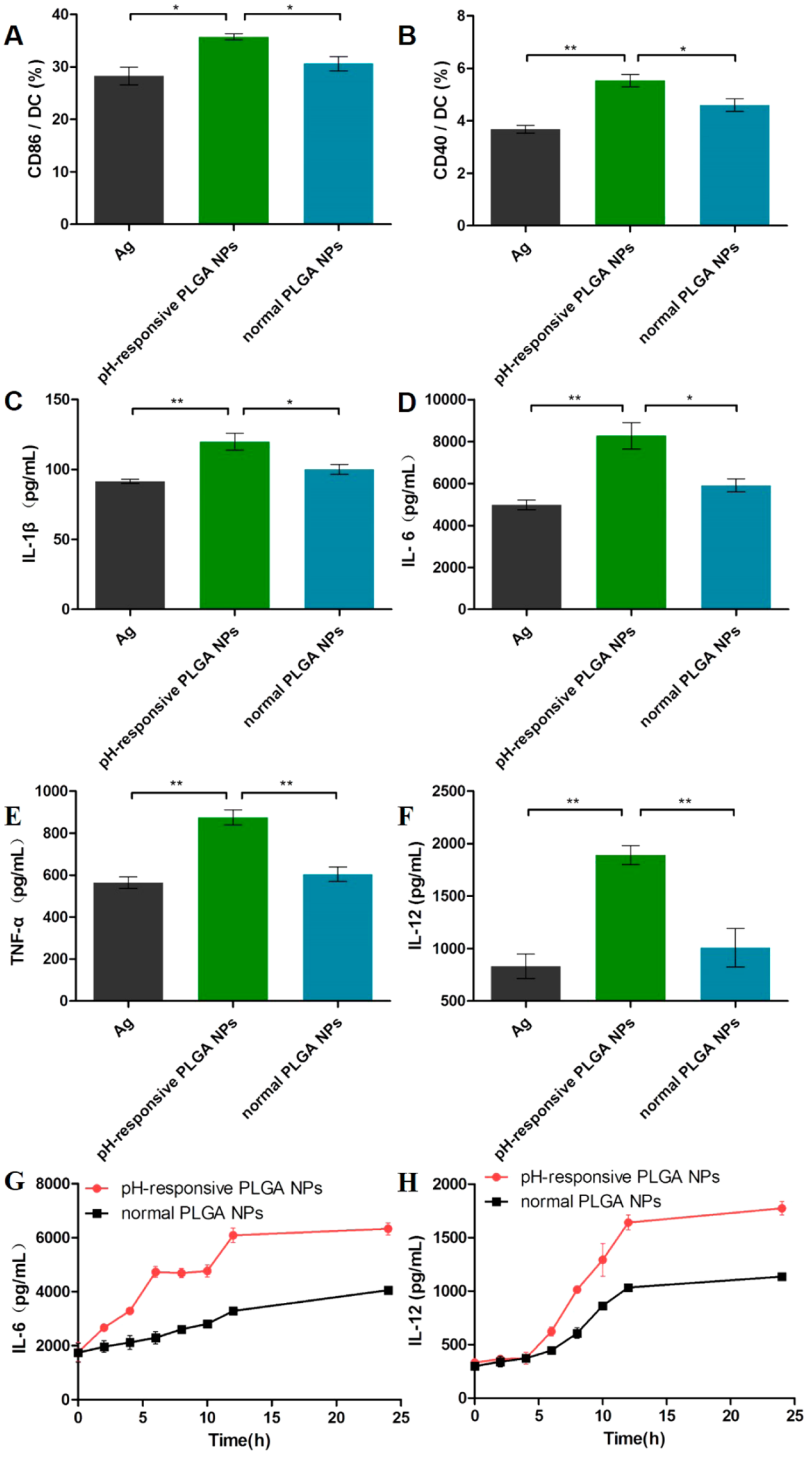

Figure 3. Expression of the co-stimulatory molecules CD86 and CD40 on DCs stimulated with NPs. DCs were stimulated for 24 h, then harvested, stained with anti-CD11c antibody, and analyzed for $CD86^+CD11c^+$ or $CD40^+CD11c^+$ cell percentages within the gated $CD11c^+$ cell population. Percentages of (A) $CD86^+CD11c^+$ and (B) $CD40^+CD11c^+$ cells were analyzed. Data are expressed as means ± SEM ($n = 6$). (C–F) Cytokine (IL-1β, IL-6, TNF-α, and IL-12) release of BMDCs stimulated with NPs for 24 h. Cytokine release of (G) IL-6 and (H) IL-12 at dictated time points. Data are expressed as means ± SEM ($n = 6$) (*$p < 0.05$; **$p < 0.01$; ***$p < 0.001$).

intervals. On day 14 after priming, titers of all groups were low, but pH-responsive PLGA NPs were higher than other groups. The weakest response, immunized with antigen alone, was almost below the detection limit. On day 21, such differences still existed, and IgG titers with NPs increased slightly. At this time point, pH-responsive PLGA NPs produced maximum titers compared to the normal NPs group and antigen alone. A second immunization boosted titers for all groups. On day 28, IgG titers treated with pH-responsive PLGA

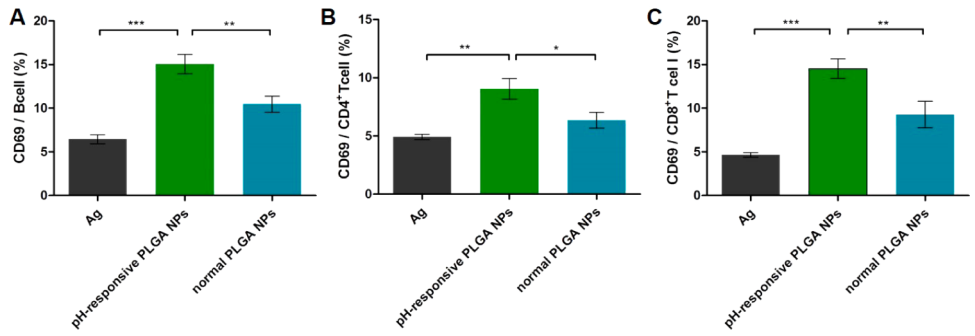

Figure 4. Frequency of CD69$^+$ of B cells and T cells evaluated by FACS. Data are expressed as means ± SEM (n = 6) (*p < 0.05; **p < 0.01; ***p < 0.001).

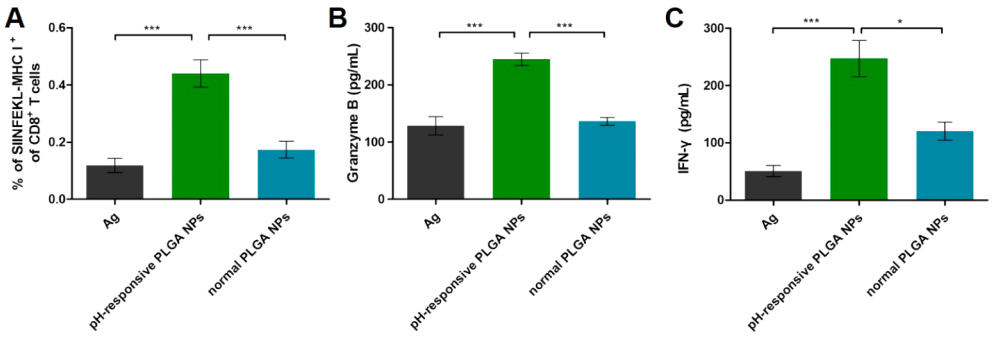

Figure 5. Evaluation of effector T cell immune response. (A) Numbers of SIINFEKL-MHC I$^+$ CD8$^+$ T cells using the antigenic peptide-MHC pentamer staining method. (B, C) Cytokine release of splenocytes from immunized C57BL/6 mice restimulated *ex vivo*. Data are expressed as means ± SEM (n = 6) (*p < 0.05; **p < 0.01; ***p < 0.001).

NPs increased to 4.167 (log 10), followed by alum, normal PLGA NPs, and antigen alone. The booster vaccination produced the highest IgG titers for all groups. On day 35, titers induced by pH-responsive PLGA NPs increased more, by 1000%, 3900%, and 6300% of titers compared with alum, normal PLGA NPs, and antigen alone (Figure 7A).

Next, we measured the effect of NP-based adjuvants on Th1 and Th2 cell polarization. IgG subclass switching is regulated by Th cells (IgG2a is directed by Th1 cells; IgG1 is directed by Th2 cells).[32] Here, sera collected on the day of animal sacrifice were assessed for IgG2a/IgG1 (Figure 7B). The significantly higher ratio of IgG2a/IgG1 (p < 0.05) revealed that pH-responsive NPs induced Th1 polarization. These data were consistent with greater IFN-γ production, which was representative of Th1 cytokines.

DISCUSSION

Compared with traditional vaccine adjuvants such as alum, NP-based adjuvants were potent for inducing cell-mediated immune responses to cytotoxic damage.[33] Previously, investigators have utilized PLGA NPs as a promising tool for inducing an immune response, but the immune potency was still limited.[12,13] Thus, we created PLGA NPs that could release antigens intracellularly rapidly in response to DC pH. These NPs had thin shells and large cavities to enable disintegration and encapsulated NH_4HCO_3, which promoted antigen release while ensuring antigen integrity and antigenicity. Our previous research found that normal PLGA NPs were shown to have a certain degree of cell-mediated responses by the lysosome escape and cross-presentation of antigens.[11] Recently, researchers proved that the slow release of antigens from PLGA NPs might more closely approximate the presence of soluble antigens during infection, which would not be optimal,[34,35] so their prolonged antigen release offered antigen persistence during infection that correlated with a T cell response.[11,36,37] Cross-presentation of NP-based antigens involved antigen internalization, trafficking through the endocytic compartment, antigenic peptide generation, and peptide loading onto MHC class I molecules. Recent studies suggested that active alkalization of phagosomes was required for cross-presentation,[38] but this phenomenon was transient. When antigens could be processed for cross-presentation, ROS production ceased, resulting in phagosome acidification and activation of lysosomal proteases.[39] This permitted generation of peptides from antigens within the phagosomes, which then could be loaded onto MHC II molecules.[40] Hence, NP-based antigen events occurred sequentially: first, cross-presentation occurred, and then antigens were loaded onto MHC II molecules. With a view to this question, our pH-responsive PLGA NPs with rapid antigen release behaviors could amplify cross-presentation aiming at enhancing the cellular immune response. We observed

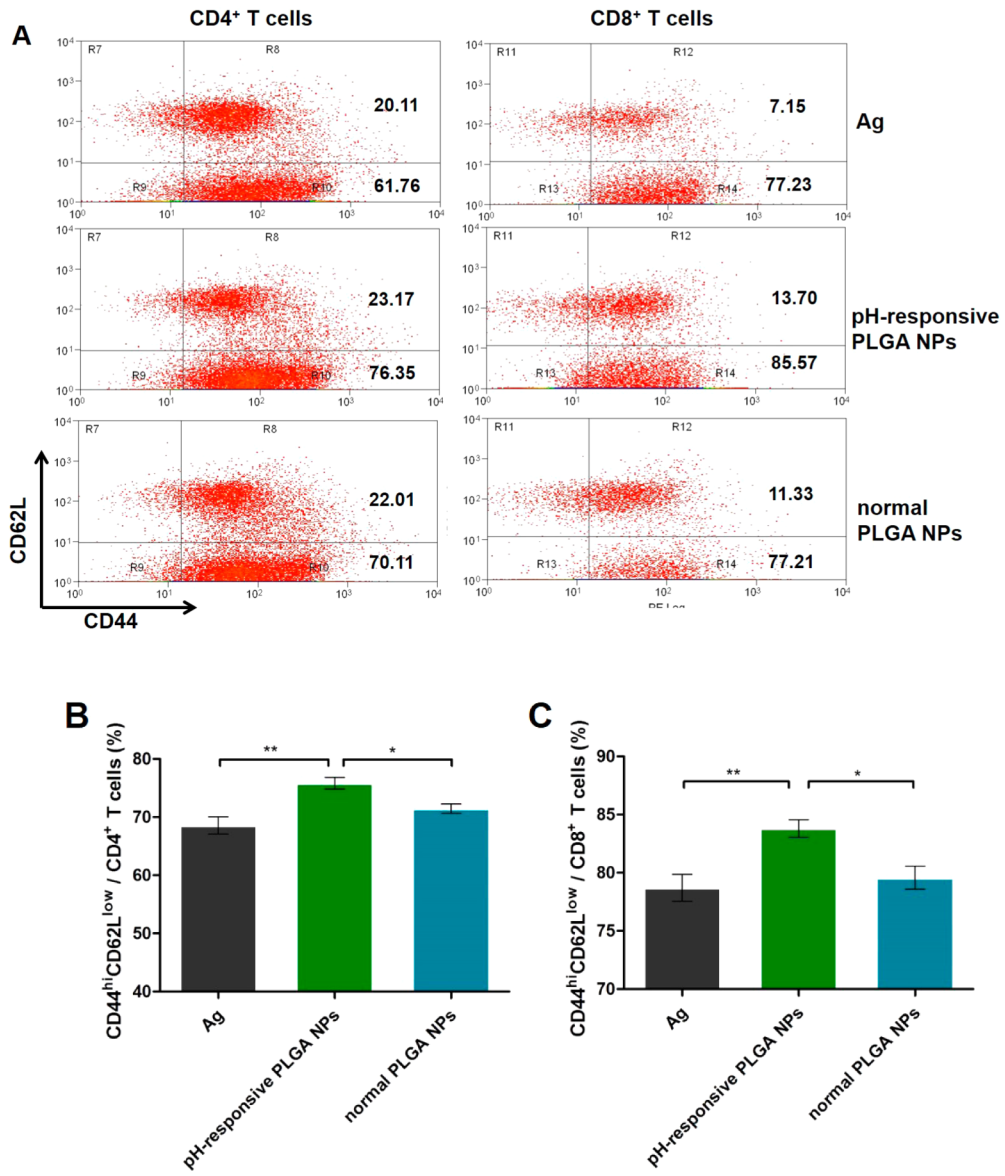

Figure 6. Frequency of central ($CD44^{hi}CD62L^{hi}$)/effector ($CD44^{hi}CD62L^{low}$) memory $CD4^+$ and $CD8^+$ T cells. Mice ($n = 6$) were immunized three times as described in the Method section. Splenocytes were harvested on day 35 after the first immunization and stimulated *ex vivo* with antigen for 72 h. The frequency of $CD44^{hi}CD62L^{hi}$ /$CD4^+$ T cells, $CD44^{hi}CD62L^{low}$/$CD4^+$ T cells, $CD44^{hi}CD62L^{hi}$/ $CD8^+$ T cells, and $CD44^{hi}CD62L^{low}$ /$CD8^+$ T cells were measured by flow cytometry. FACS plots in (A) are representative of the mean percentages of six mice in each group. Data of (B) $CD44^{hi}CD62L^{low}$/$CD4^+$ T cells and (C) $CD44^{hi}CD62L^{low}$/$CD8^+$ T cells are expressed as means ± SEM ($n = 6$) (*$p < 0.05$; **$p < 0.01$; ***$p < 0.001$).

that pH-responsive NP-based antigens possessed excellent endosome-escape ability and the highest cross-presentation frequency in the widely accepted *in vitro* B3Z assays. However, the exact location of antigen release (early endosomes, late endosomes, and lysosomes) was uncertain, and this would be a subject of future research.

Priming and polarization of T and B cell responses required not only the presentation of antigenic entities but also the expression of co-stimulatory molecules and production of cytokines by DCs. Specifically, TNF-α and IL-12p70 were greatly stimulated by pH-responsive PLGA NPs, which suggested that a Th1-like response occurred. Also, secretion of pro-inflammatory cytokines, IL-6 and IL-1β, which was associated with the NRLP3 inflammasome, suggested that pH-responsive PLGA NP-based vaccine adjuvants could activate DCs in a way that was potentially inflammatory. The stimulation of DCs by pH-responsive PLGA NP-based vaccine adjuvants was time-dependent. The rapid and tremendous secretion of cytokines stimulated by pH-responsive PLGA NPs could activate and potentiate $CD8^+$ T cells.[28] Thus, pH-responsive PLGA NP-based vaccine adjuvants not only guided antigens for cross-presentation but also boosted the immune response by efficiently activating and maturing APCs.[41,42]

Vaccine potency tests were conducted in mice. Compared with antigen, alum, and normal PLGA NPs,

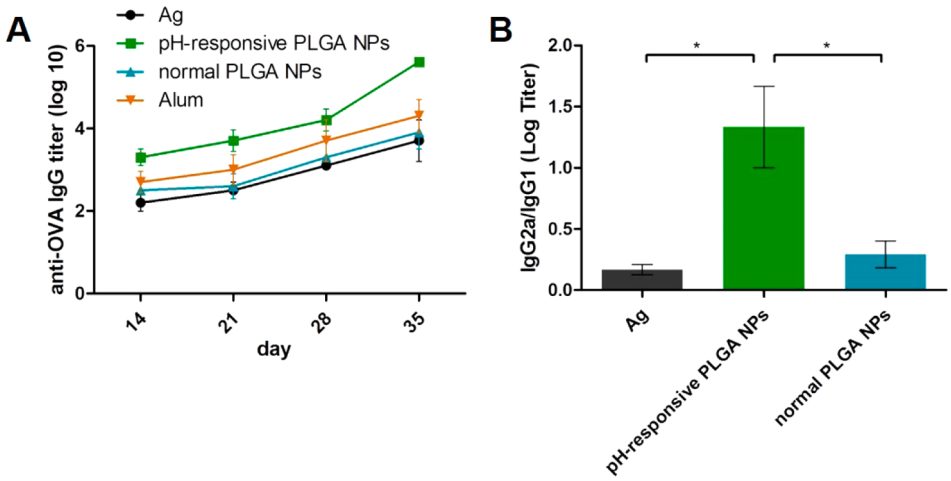

Figure 7. Production of antigen-specific antibodies in the sera of C57BL/6 mice. (A) Antigen-specific IgG titers of indicated time points. (B) Ratio of IgG2a/IgG1. Data are expressed as means ± SEM ($n = 6$) (*$p < 0.05$; **$p < 0.01$; ***$p < 0.001$).

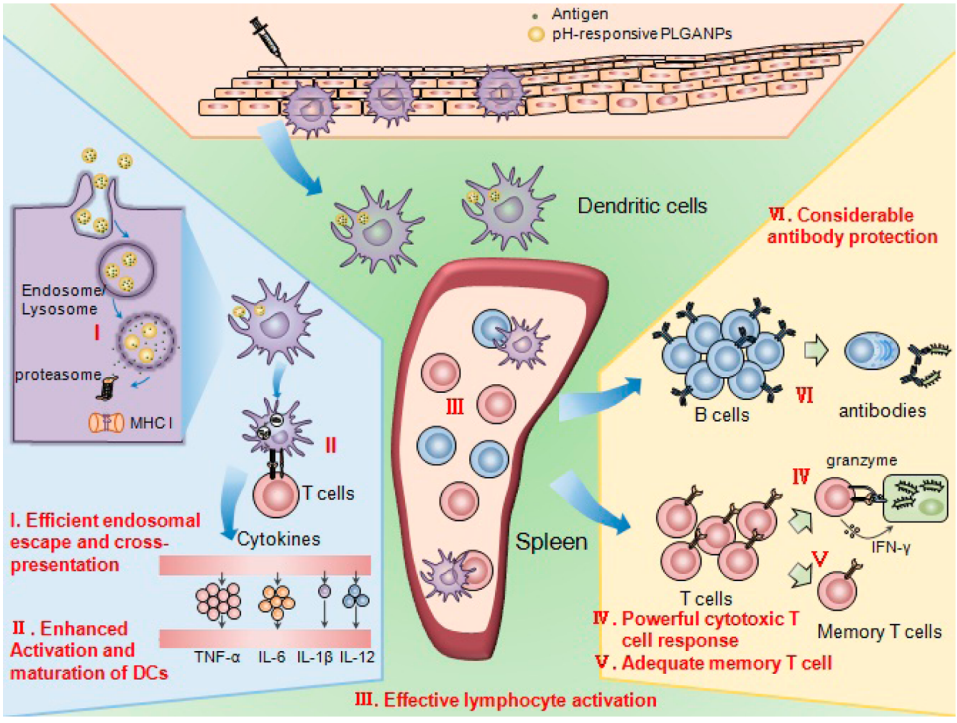

Figure 8. Schematic illustration of the proposed mode of action of pH-responsive PLGA NPs.

pH-responsive NPs augmented anti-OVA antibody responses, which might be attributed to their immunostimulatory effects of DC activation and maturation. Surprisingly, pH-responsive NPs potently enhanced secondary IgG2a. Rapid antigen release produced by pH-responsive PLGA NPs increased the probability of antigens interacting with T and B cell responses in immunological synapses, facilitating subclass switching.[30] The IgG2a/IgG1 ratio suggested that pH-responsive NPs promoted Th1-like responses. The efficacy of pH-responsive NP-based vaccine adjuvants for stemming and eliminating intracellular pathogens had been increased through enhanced CTL, but this was based on better cross-presentation of exogenously delivered antigens. In the effector phase after immunization with pH-responsive PLGA NPs, a large pool of antigen-specific $CD8^+$ T cells was recruited. CTLs of mice immunized with these NPs secreted effector cytokines such as IFN-γ and granzyme B in response to antigenic stimulation.

Another goal of vaccination was to generate long-lived immunological memory that protected hosts from reinfection of specific intracellular pathogens.[43] A component of immunological memory was cellular immunity (mostly memory $CD8^+$ T cells).[44] Our pH-responsive PLGA NP-based vaccine adjuvants favored

more memory T cell formation. First, effector memory $CD8^+$ and $CD4^+$ T cells elicited immediate effector functions in response to pathogen entry and rapidly expanded to kill the pathogens. In agreement with this idea, our data indicated that large amounts of $CD8^+$ T_{EM} and $CD4^+$ T_{EM} produced by pH-responsive PLGA NP-based vaccine adjuvants had effector phenotypes and functionality characterized by higher IFN-γ production. Also, large amounts of $CD8^+$ T_{CM} and $CD4^+$ T_{CM} guaranteed long-lasting cellular memory. pH-responsive NPs maintained the strength for forming T cell memory that was similar to that of normal PLGA NPs with controlled release behavior.[45] This rapid antigen intracellular release behavior contributed greatly to vaccine efficacy.

From the data presented here, we propose the following model to explain the underlying mode of action of pH-responsive PLGA NPs (Figure 8). First, after uptake by DCs, antigens could be released rapidly from the NPs and escape from the endosomes/lysosomes and then be cross-presented (Figure 2). Meanwhile, pH-responsive PLGA NP-based vaccine adjuvants activated and maturated DCs to prime T cells by up-regulating co-stimulatory molecules and secreting cytokines (Figure 3). Effective lymphocyte activation initiated the whole immune response (Figure 4). Then, more potent antigen-specific immune responses were elicited and memory T cell responses were maintained (Figures 5 and 6). As well as T cell responses, B cells produced adequate antibody protection (Figure 7). Therefore, pH-responsive PLGA NPs enhanced antigen-specific immune responses, which especially achieved better cellular immunity to eliminate intracellular pathogens.

CONCLUSIONS

Here we offered proof-of-concept that pH-responsive PLGA NPs could rapidly release antigens, and these safe and biocompatible NPs might be suitable for vaccine delivery. Our NPs could deliver antigens to the cytoplasm, cross-present them, and activate and mature DCs to induce humoral and strong cellular immune responses. These effects were also "remembered" by the immune system. This work was novel because pH-responsive PLGA NP-based vaccine adjuvants with rapid antigen release behavior could cross-present antigens and increase the quality and magnitude of the vaccine response.

MATERIALS AND METHODS

Materials and Reagents. With a lactic/glycolic molar ratio of 75:25 and an inherent viscosity of 0.16 dL/g, PLGA was obtained from Lakeshore (Westerville, OH, USA). Ovalbumin and organic solvents were purchased from Sigma (St. Louis, MO, USA). Poly(vinyl alcohol) (PVA-217, degree of polymerization 1700, degree of hydrolysis 88.5%), used as a stabilizer in an outer water phase, was provided by Kuraray (Tokyo, Japan). SPG membranes (Shirasu Porous Glass) with pore sizes of 2.9 and 5.3 μm were used in this study. NH_4HCO_3 (analytical grade) was purchased from Beijing Chemical Works. Premixed membrane emulsification (FMEM-50M) was provided by National Engineering Research Center for Biotechnology (Beijing, China). Concanavalin A was from Roche (Germany). Roswell Park Memorial Institute (RPMI) 1640, Dulbecco's modified Eagle medium (DMEM), and fetal bovine serum (FBS) were purchased from Gibco (Grand Island, NY, USA). Alexa 635-phalloidin and LysoTracker probes were from Invitrogen (Grand Island, NY, USA). FITC was purchased from Sigma-Aldrich. Fluorochrome-labeled MHC II, CD86, CD80, CD11c, CD69, CD44, CD62L, CD4, CD8, CD19, and CD3 antibodies were purchased from eBioscience (San Diego, CA, USA). Recombinant mouse GM-CSF and IL-4 were obtained from Peprotech (Rocky Hill, NJ, USA). Mouse cytokine ELISA kits were purchased from eBioscience. OVA-derived (H-2Kb, SIINFEKL) specific MHC I pentamers were purchased from ProImmune (Oxford, UK).

Fabrication and Characterization of OVA-Containing PLGA NP-Formulated Vaccine. Uniform-sized PLGA NPs were prepared by combining the emulsion−diffusion−extraction approach and premixed emulsification technique. For pH-responsive PLGA NPs, 100 mg of OVA was dissolved in 5 mL of water, which was already added to 12.5 mg of NH_4HCO_3 (aqueous phase), and 0.33 g of PLGA was dissolved in 10 mL of ethyl acetate (organic phase). Subsequently, 5 mL of the aqueous and 10 mL of the organic phase were mixed and homogenized under 7500 rpm for 30 s in an ice bath to obtain the primary W/O emulsion. Then, the primary emulsion was added to 75 mL of aqueous PVA (1.9%) and stirred at 400 rpm for 2 min using a magnetic stirrer (IKA, Germany) to form the W/O/W double-emulsion, which was then transferred into the premix reservoir. Subsequently, uniform-sized nanodroplets were achieved by repeatedly extruding the emulsions through the membrane pores under high pressure. After that, the resultant double-emulsion was transferred into 900 mL of water that contained 0.9% NaCl, and the mixture stirred for 4 h at room temperature to extract ethyl acetate and solidify the NPs. The obtained NPs were collected by centrifugation (4000*g*, 10 min), washed three times with ultrapure (UP) water, and freeze-dried for storage. For injection, the NPs were dispersed in phosphate-buffered saline (PBS).

To observe the shape and surface morphology, NPs were resuspended in UP water, coated with gold using a gold sputter in a high-vacuum evaporator, and observed using a JSM-6700F scanning electron microscopy (JEOL, Japan). To observe the inner structure, NPs were prepared by dropping a dispersed solution on a carbon film supported by a copper grid (230-mesh, Beijing Zhongjingkeyi Technology Co. Ltd.), dried, and then observed using a JEM-1400 transmission electron microscope operated at 80 kV (JEOL, Japan). For size and zeta potential measurements, NPs were analyzed using a NanoSizer ZS (Malvern Instruments, Malvern UK). To confirm NH_4HCO_3 encapsulation, XRD patterns were obtained using an X'Pert-PRO MPD powder diffractometer (PANalytical, The Netherlands).

NP-encapsulated OVA content was measured in triplicate by incubating approximately ~10 mg of NPs in 5 mL of a solution of 0.1 M sodium hydroxide at room temperature overnight and assaying protein using a Micro BCA protein assay kit (Pierce). NP-encapsulated OVA release profiles *in vitro* were obtained by immersing NPs in test tubes containing 10 mL of PBS with different pH values (pH 7.4, 6.5, 5.0). pH-responsive PLGA NP-encapsulated OVA release profiles *in vitro* were obtained by immersing NPs in test tubes containing 10 mL of PBS with pH values of 6.5 and 5.0. Indicated amounts of proton scavenger (sodium hydroxide) were added at indicated times (1, 2, and 8 h) to neutralize the acids and raise the pH to 7.4. For the test medium with pH values of 5.0 and 6.5, 47 and 35 μL of a solution of 2 M sodium hydroxide were added, respectively. Test tubes were gently shaken in a thermostatic rotary shaker (100 rpm, 37 °C). Samples were then removed at predetermined time

points, and an equal amount of the same medium was added to maintain a constant volume. Next, OVA released from the NPs was measured using a Micro BCA protein assay kit. Finally, test NPs received were examined by SEM.

Far-UV circular dichroism (CD) (190−250 nm) was used to monitor changes in antigen secondary structures encapsulated in pH-responsive PLGA NPs. All CD spectra were collected on a Jasco J-810 (Easton, MD, USA) instrument with a 1 cm quartz cell. Using Jasco software, the background solution (polymer degradation product in deionized water) was subtracted from each protein spectrum. A minimum of three protein spectra were collected per sample and averaged. To detect changes in the tertiary structure of antigens encapsulated in the pH-responsive PLGA NPs, fluorimetry was performed (F-4500 fluorescence spectrometer, Hitachi, Japan). The emission spectrum (300−450 nm) of each sample was collected at an excitation wavelength of 280 nm. When excited at 280 nm, the emission spectrum was a result of contributions from protein tryptophan and tyrosine residues.[46] Each protein spectrum was corrected by subtracting the spectrum of the appropriate blank solution (no protein).

The adsorption−desorption isotherms and BET specific surface area were measured by nitrogen with an ASAP 2010 accelerated surface area and porosimetry system (Norcross, GA, USA). Briefly, weighed amounts of NPs were placed in the glass cells and outgassed with nitrogen at 30 °C for 4 h before analysis. Subsequently, the sample and the reference cells were immersed in liquid nitrogen at −196 °C, and isotherms were obtained from the volume of nitrogen adsorbed/desorbed onto the surface of NPs as a function of relative pressure. The adsorption−desorption isotherms and BET specific surface area of NPs were obtained using ASAP 2010 software.

Endotoxin Levels. The endotoxin level in the final formulation was determined by the LAL assay method with a commercially available endotoxin assay kit (Pyrosate 0.25 EU/mL) from Associates of Cape Cod (Falmouth, MA, USA). According to the manufacturer's instructions, the endotoxin levels of all formulations were tested, and the levels were less than 0.05 EU/mg NPs. All materials used were sterile, and the endotoxin levels were also less than 0.05 EU/mL.

Antigen Uptake and Intracellular Localization by BMDCs *in Vitro*. BMDCs were cultured from bone marrow cells using an established protocol.[47] In brief, bone marrow cells were isolated from C57BL/6 mouse femurs and tibias and cultured in RPMI medium 1640 supplemented with GM-CSF and IL-4 (10 and 50 ng/mL, respectively) at 37 °C for 6 days to harvest immature DCs. For antigen uptake, immature DCs were cultured with FITC (Sigma-Aldrich)-conjugated OVA or NP-encapsulated FITC-OVA at 37 °C for a specific time. Cells were then washed twice with PBS (10 mM, pH 7.4) and stained with anti-CD11c antibody diluted with flow cytometry staining buffer (eBioscience) to specifically identify DCs. The percentage of $CD11c^+FITC\text{-}OVA^+$ cells on gated $CD11c^+$ cells was measured using a Beckman Coulter CyAnTM ADP flow cytometer and analyzed using Summit software (version 4.3).

Cell viability was assessed using the colorimetric cell counting kit-8 (CCK-8) from Dojindo Laboratories (Kyoto, Japan). CCK-8 is based on a colorimetric assay utilizing a highly water-soluble tetrazolium salt, WST-8 [2-(2-methoxy-4-nitrophenyl)-3-(4-nitrophenyl)-5-(2,4-disulfophenyl)-^{2}H-tetrazolium, monosodium salt]. To assess cell viability, cells were plated in 96-well plates at a density of 1×10^5 cells in 150 μL of growth medium per well. The wells were then treated with 50 μL of different concentrations of pH-responsive PLGA NP solutions diluted in growth medium. After 24 h, 10 μL of CCK-8 reagent was added to each well and incubated at 37 °C for 4 h. Absorbance at 450 nm was measured, and the results were calculated from the ratio of the average OD_{450} values of wells containing NP-stimulated cells to the average OD_{450} values of wells containing only cells with medium.

To evaluate antigen intracellular localization in DCs, immature DCs were plated onto a poly-D-lysine-coated Petri dish for 1 h, and nonadherent DCs were removed. FITC-OVA and NPs-encapsulated-FITC-OVA were added into the Petri dish. For inhibition of lysosomal acidification, DCs were incubated with 100 μM chloroquine (tlrl-chql; InvivoGen) (San Diego, CA, USA) for 1 h before adding the pH-responsive PLGA NP-encapsulated-FITC-OVA. After 16 h of incubation, the cells were washed three times in PBS (10 mM, pH 7.4). To label the lysosomes, cells were incubated in prewarmed media (37 °C) containing LysoTracker-Red DND-99 (Molecular Probes-Invitrogen, CA, USA). The corresponding fluorescent images were obtained using CLSM TCS SP5 (Leica, Germany).

Activation and Maturation of BMDCs by NPs *in Vitro*. Immature DCs were stimulated with soluble OVA or OVA-containing NPs for a specified time and labeled with fluorochrome-labeled antibodies diluted with flow cytometry staining buffer against CD86 and CD40. CD86 and CD40 expression on BMDCs was measured by cytometry as depicted above. Cytokines in culture supernatants of BMDCs were quantified by using mouse IL-6, IL-12p70, IL-1β, and TNF-α ELISA kits according to the manufacturer's protocol (eBioscience) and calculated using a five-parameter curve obtained from the absorbance values of standards provided by the manufacturer.

Detection of Antigen Presentation with a LacZ T Cell Hybridoma Assay. Antigen cross-presentation of $OVA_{257-264}$ was detected using a $CD8^+$ T cell hybridoma B3Z cell line that expressed β-galactosidase under control of the IL-2 promoter.[27] B3Z cells were kindly provided by Prof. Bin Gao and Prof. Juan Ma from Institute of Microbiology, Chinese Academy of Sciences (Beijing). Hybridoma cells (1×10^5) were incubated with BMDCs (2×10^5) per well of a 96-well plate. Cells were co-incubated with indicated amounts of NP-encapsulated antigens. After 18 h of incubation at 37 °C, in 5% CO_2, plates were washed with PBS, and 100 μL of LacZ buffer [0.13% Nonidet P-40, 9 mM $MgCl_2$, 0.15 mM chlorophenol red-β-D-galactopyranoside (Roche) in PBS] was added for up to 4 h at 37 °C. Absorbance was measured at 570/620 nm using a microplate reader (Tecan, Germany).

Animals and Immunization. Specific-pathogen-free female C57BL/6 mice were purchased from the Beijing Laboratory Animal Center and housed in a specific-pathogen-free facility. Mice (4−6 weeks of age) were used for DC isolation. Mice (6−8 weeks of age) ($N = 6$ mice/group) were immunized with a 100 μL suspension of NP (pH-responsive PLGA NPs, normal PLGA NPs)-encapsulated OVA in PBS, PBS plus OVA, or aluminum plus OVA by im injection on days 0, 14, and 28. On days 14, 21, 28, and 35 after the first immunization, sera were collected from the venous plexus of mice's posterior orbits for antibody analysis. Mice were sacrificed to collect spleens for immunological tests on day 35. All animals were treated according to the regulations of Chinese law and the local Ethical Committee.

Antigen-Specific IgG Determination by ELISA. Serum was harvested from blood after clotting at RT and centrifugation. ELISA plates (96-well) were coated with 2 μg per well of OVA in coating buffer (50 mM Na_2CO_3−$NaHCO_3$, pH 9.6) overnight at 4 °C. After washing six times with PBS−0.05% Tween 20 (v/v), the plates were blocked with 1% (w/v) BSA in PBS for 90 min at 37 °C. The concentration of antigen-specific IgG in sera was monitored using a 2-fold dilution series beginning at an initial 100-fold dilution. Plates were incubated at 37 °C for 1 h and washed six times with PBS−0.05% Tween 20. The HRP-conjugated anti-mouse antibody (Abcam) was then added into each well at a 1:10 000 dilution and incubated at 37 °C for 40 min. Plates were washed six times and developed with TMB solution in the dark for 15 min. The enzymatic reaction was stopped by adding 2 M H_2SO_4, and the OD_{450} values were read using a microplate reader. End-point titers were shown as the sample dilution resulting in an OD_{450} equal to twice the mean background (negative serum) of the assay.

Cytokine Measurements and Granzyme Expression in Restimulated Splenocytes with ELISA. Next, 35 days after the first immunization, spleens were harvested, and splenocytes were prepared by mincing against a 200-mesh cell strainer. Erythrocytes were lysed by 0.9% ammonium chloride, and splenocytes were washed three times with RPMI 1640. Splenocytes (4×10^6) were cultured with OVA (50 μg/mL) or concanavalin A (1 mg/mL) as a positive control at 37 °C, 5% CO_2, and 95% humidity. Supernatants were harvested at 72 h and stored at −70 °C until analyzed. Granzyme B and IFN-γ cytokine were measured with ELISA

kits according to the manufacturer's protocol (eBioscience). Cytokines in supernatants were calculated using a five-parameter curve obtained from the absorbance values of standards provided by the manufacturer.

Evaluation of Lymphocyte Activation and T Cell Response by Flow Cytometry. Flow cytometry was performed to evaluate the effect of pH-responsive PLGA NPs on lymphocyte activation, memory T cell response, and antigen-specific $CD8^+$ T cell response. C57BL/6 mice ($n = 6$) were intramuscularly vaccinated twice at a 2-week interval. On day 35 after the first immunization, mice were euthanized, and splenocytes were harvested and stimulated with OVA (OVA, 50 μg/mL; splenocytes, 5.0×10^6 cells/mL) for 72 h in a 37 °C humidified incubator with 5% CO_2. After washing, cells were stained with fluorescent-labeled anti-mouse antibodies against CD4, CD8, CD19, CD69, CD44, and CD62L (eBioscience) and peptide-MHC pentamers (PE-labeled SIINFEKL/H-$2K^b$ pentamer, Proimmune, UK). A CyAn ADP flow cytometer measured the percentages of activated lymphocytes ($CD69^+$), effector memory T cells ($CD44^{hi}CD62L^{low}$), central memory T cells ($CD44^{hi}CD62L^{hi}$), and antigen-specific $CD8^+$ T cells ($CD8^+$ SIINFEKL-MHC I^+). Data analysis was performed using Summit software.

Statistical Analysis. All statistical analyses were performed using GraphPad Prism 5 software (San Diego, CA, USA). Results were expressed as means ± SEM. Differences between two groups were tested using an unpaired, two-sided Student's *t* test. Differences among more than two groups were evaluated by one-way ANOVA with significance determined by Tukey-adjusted *t*-tests.

Conflict of Interest: The authors declare no competing financial interest.

Acknowledgment. The authors thank Prof. B. Gao and Prof. J. Ma for kindly providing the B3Z T cell hybridoma. This work was financially supported by the National Science Foundation of China (Grant No. 21476243), 973 Program (Grant No. 2013CB531500), the 863 Program (Grant No. 2012AA02A406), and the Knowledge Innovation Program of the Chinese Academy of Sciences (Grant No. KSCX2-EW-R-19).

Supporting Information Available: The Supporting Information file includes fluorescent and CD spectra of antigen, N_2 adsorption−desorption isotherm of NPs, SEM micrograph showing morphological changes in NPs during the course of antigen release in media with different pH values, effect of NPs on BMDC viability, antigen uptake by BMDCs, representative graph of frequency of $CD69^+$ on B cells and T cells, and representative graph of frequency of pentamer-staining SIINFEKL-MHC I^+ on $CD8^+$ T cells. This material is available free of charge *via* the Internet at http://pubs.acs.org.

REFERENCES AND NOTES

1. Mahmoud, A. A. Tropical Medicine. Current Problems and Possible Solutions. *Infect. Dis. Clin. N. Am.* **1995**, *9*, 265–274.
2. Gherardi, R. K.; Coquet, M.; Cherin, P.; Belec, L.; Moretto, P.; Dreyfus, P. A.; Pellissier, J. F.; Chariot, P.; Authier, F. J. Macrophagic Myofasciitis Lesions Assess Long-Term Persistence of Vaccine-Derived Aluminium Hydroxide in Muscle. *Brain* **2001**, *124*, 1821–1831.
3. Petrovsky, N.; Aguilar, J. C. Vaccine Adjuvants: Current State and Future Trends. *Immunol. Cell Biol.* **2004**, *82*, 488–496.
4. Kool, M.; Fierens, K.; Lambrecht, B. N. Alum Adjuvant: Some of the Tricks of the Oldest Adjuvant. *J. Med. Microbiol.* **2012**, *61*, 927–934.
5. Gupta, R. K.; Relyveld, E. H.; Lindblad, E. B.; Bizzini, B.; Ben-Efraim, S.; Gupta, C. K. Adjuvants−A Balance between Toxicity and Adjuvanticity. *Vaccine* **1993**, *11*, 293–306.
6. Gupta, R. K.; Rost, B. E.; Relyveld, E.; Siber, G. R. Adjuvant Properties of Aluminum and Calcium Compounds. *Pharm. Biotechnol.* **1995**, *6*, 229–248.
7. Gupta, R. K. Aluminum Compounds as Vaccine Adjuvants. *Adv. Drug Delivery Rev.* **1998**, *32*, 155–172.
8. Leleux, J.; Roy, K. Micro and Nanoparticle-Based Delivery Systems for Vaccine Immunotherapy: An Immunological and Materials Perspective. *Adv. Healthcare Mater.* **2012**, *2*, 72–94.
9. Peek, L. J.; Middaugh, C. R.; Berkland, C. Nanotechnology in Vaccine Delivery. *Adv. Drug Delivery Rev.* **2008**, *60*, 915–928.
10. Wang, Y. Q.; Wu, J.; Fan, Q. Z.; Zhou, M.; Yue, Z. G.; Ma, G. H.; Su, Z. G. Novel Vaccine Delivery System Induces Robust Humoral and Cellular Immune Responses Based on Multiple Mechanisms. *Adv. Healthcare Mater.* **2014**, *3*, 670–681.
11. Yue, H.; Wei, W.; Fan, B.; Yue, Z.; Wang, L.; Ma, G.; Su, Z. The Orchestration of Cellular and Humoral Responses Is Facilitated by Divergent Intracellular Antigen Trafficking in Nanoparticle-Based Therapeutic Vaccine. *Pharmacol. Res.* **2012**, *65*, 189–197.
12. Hamdy, S.; Haddadi, A.; Shayeganpour, A.; Samuel, J.; Lavasanifar, A. Activation of Antigen-Specific T Cell-Responses by Mannan-Decorated PLGA Nanoparticles. *Pharm. Res.* **2011**, *28*, 2288–2301.
13. Cruz, L. J.; Tacken, P. J.; Fokkink, R.; Joosten, B.; Stuart, M. C.; Albericio, F.; Torensma, R.; Figdor, C. G. Targeted PLGA Nano- but Not Microparticles Specifically Deliver Antigen to Human Dendritic Cells *via* DC-Sign *in Vitro*. *J. Controlled Release* **2010**, *144*, 118–126.
14. Scott, C. J.; Marouf, W. M.; Quinn, D. J.; Buick, R. J.; Orr, S. J.; Donnelly, R. F.; McCarron, P. A. Immunocolloidal Targeting of the Endocytotic Siglec-7 Receptor Using Peripheral Attachment of Siglec-7 Antibodies to Poly(Lactide-co-Glycolide) Nanoparticles. *Pharm. Res.* **2008**, *25*, 135–146.
15. Chen, X.; Liu, Y.; Wang, L.; Liu, Y.; Zhang, W.; Fan, B.; Ma, X.; Yuan, Q.; Ma, G.; Su, Z. Enhanced Humoral and Cell-Mediated Immune Responses Generated by Cationic Polymer-Coated PLA Microspheres with Adsorbed HBsAg. *Mol. Pharmaceutics* **2014**, *11*, 1772–1784.
16. Banchereau, J.; Briere, F.; Caux, C.; Davoust, J.; Lebecque, S.; Liu, Y. J.; Pulendran, B.; Palucka, K. Immunobiology of Dendritic Cells. *Annu. Rev. Immunol.* **2000**, *18*, 767–811.
17. Trombetta, E. S.; Mellman, I. Cell Biology of Antigen Processing *in Vitro* and *in Vivo*. *Annu. Rev. Immunol.* **2005**, *23*, 975–1028.
18. Guermonprez, P.; Valladeau, J.; Zitvogel, L.; Thery, C.; Amigorena, S. Antigen Presentation and T Cell Stimulation by Dendritic Cells. *Annu. Rev. Immunol.* **2002**, *20*, 621–667.
19. Swartz, M. A.; Hubbell, J. A.; Reddy, S. T. Lymphatic Drainage Function and Its Immunological Implications: From Dendritic Cell Homing to Vaccine Design. *Semin. Immunol.* **2008**, *20*, 147–156.
20. Wykes, M.; Pombo, A.; Jenkins, C.; MacPherson, G. G. Dendritic Cells Interact Directly with Naive B Lymphocytes to Transfer Antigen and Initiate Class Switching in a Primary T-Dependent Response. *J. Immunol.* **1998**, *161*, 1313–1319.
21. Joffre, O. P.; Segura, E.; Savina, A.; Amigorena, S. Cross-Presentation by Dendritic Cells. *Nat. Rev. Immunol.* **2012**, *12*, 557–569.
22. Basta, S.; Alatery, A. The Cross-Priming Pathway: A Portrait of an Intricate Immune System. *Scand. J. Immunol.* **2007**, *65*, 311–319.
23. Ruff, L. E.; Mahmoud, E. A.; Sankaranarayanan, J.; Morachis, J. M.; Katayama, C. D.; Corr, M.; Hedrick, S. M.; Almutairi, A. Antigen-Loaded pH-Sensitive Hydrogel Microparticles Are Taken up by Dendritic Cells with No Requirement for Targeting Antibodies. *Integr. Biol.* **2013**, *5*, 195–203.
24. Thiele, L.; Diederichs, J. E.; Reszka, R.; Merkle, H. P.; Walter, E. Competitive Adsorption of Serum Proteins at Microparticles Affects Phagocytosis by Dendritic Cells. *Biomaterials* **2003**, *24*, 1409–1418.
25. Nguyen, D. N.; Green, J. J.; Chan, J. M.; Longer, R.; Anderson, D. G. Polymeric Materials for Gene Delivery and DNA Vaccination. *Adv. Mater.* **2009**, *21*, 847–867.
26. Hirosue, S.; Kourtis, I. C.; van der Vlies, A. J.; Hubbell, J. A.; Swartz, M. A. Antigen Delivery to Dendritic Cells by Poly(Propylene Sulfide) Nanoparticles with Disulfide Conjugated

Peptides: Cross-Presentation and T Cell Activation. *Vaccine* **2010**, *28*, 7897–7906.
27. Karttunen, J.; Sanderson, S.; Shastri, N. Detection of Rare Antigen-Presenting Cells by the Lacz T-Cell Activation Assay Suggests an Expression Cloning Strategy for T-Cell Antigens. *Proc. Natl. Acad. Sci. U.S.A.* **1992**, *89*, 6020–6024.
28. Schenkel, J. M.; Fraser, K. A.; Vezys, V.; Masopust, D. Sensing and Alarm Function of Resident Memory $CD8^+$ T Cells. *Nat. Immunol.* **2013**, *14*, 509–513.
29. Brewer, J. M.; Conacher, M.; Hunter, C. A.; Mohrs, M.; Brombacher, F.; Alexander, J. Aluminium Hydroxide Adjuvant Initiates Strong Antigen-Specific Th2 Responses in the Absence of IL-4- or IL-13-Mediated Signaling. *J. Immunol.* **1999**, *163*, 6448–6454.
30. Purkerson, J.; Isakson, P. A Two-Signal Model for Regulation of Immunoglobulin Isotype Switching. *FASEB J.* **1992**, *6*, 3245–3252.
31. Kaech, S. M.; Wherry, E. J.; Ahmed, R. Effector and Memory T-Cell Differentiation: Implications for Vaccine Development. *Nat. Rev. Immunol.* **2002**, *2*, 251–262.
32. Woof, J. M. Tipping the Scales toward More Effective Antibodies. *Science* **2005**, *310*, 1442–1443.
33. Storni, T.; Kundig, T. M.; Senti, G.; Johansen, P. Immunity in Response to Particulate Antigen-Delivery Systems. *Adv. Drug Delivery Rev.* **2005**, *57*, 333–355.
34. Cui, W.; Joshi, N. S.; Jiang, A.; Kaech, S. M. Effects of Signal 3 during CD8 T Cell Priming: Bystander Production of IL-12 Enhances Effector T Cell Expansion but Promotes Terminal Differentiation. *Vaccine* **2009**, *27*, 2177–2187.
35. Joshi, N. S.; Cui, W.; Chandele, A.; Lee, H. K.; Urso, D. R.; Hagman, J.; Gapin, L.; Kaech, S. M. Inflammation Directs Memory Precursor and Short-Lived Effector $CD8^+$ T Cell Fates *via* the Graded Expression of T-Bet Transcription Factor. *Immunity* **2007**, *27*, 281–295.
36. Kalia, V.; Sarkar, S.; Subramaniam, S.; Haining, W. N.; Smith, K. A.; Ahmed, R. Prolonged Interleukin-2Ralpha Expression on Virus-Specific $CD8^+$ T Cells Favors Terminal-Effector Differentiation *in Vivo*. *Immunity* **2010**, *32*, 91–103.
37. Badovinac, V. P.; Messingham, K. A. N.; Jabbari, A.; Haring, J. S.; Harty, J. T. Accelerated $CD8^+$ T-Cell Memory and Prime-Boost Response after Dendritic-Cell Vaccination. *Nat. Med.* **2005**, *11*, 748–756.
38. Savina, A.; Jancic, C.; Hugues, S.; Guermonprez, P.; Vargas, P.; Moura, I. C.; Lennon-Dumenil, A. M.; Seabra, M. C.; Raposo, G.; Amigorena, S. Nox2 Controls Phagosomal pH to Regulate Antigen Processing during Crosspresentation by Dendritic Cells. *Cell* **2006**, *126*, 205–218.
39. Segal, A. W. How Neutrophils Kill Microbes. *Annu. Rev. Immunol.* **2005**, *23*, 197–223.
40. Villadangos, J. A.; Ploegh, H. L. Proteolysis in MHC Class II Antigen Presentation: Who's in Charge? *Immunity* **2000**, *12*, 233–239.
41. Zhang, Z.; Tongchusak, S.; Mizukami, Y.; Kang, Y. J.; Ioji, T.; Touma, M.; Reinhold, B.; Keskin, D. B.; Reinherz, E. L.; Sasada, T. Induction of Anti-Tumor Cytotoxic T Cell Responses through PLGA-Nanoparticle Mediated Antigen Delivery. *Biomaterials* **2011**, *32*, 3666–3678.
42. Kaech, S. M.; Wherry, E. J. Heterogeneity and Cell-Fate Decisions in Effector and Memory $CD8^+$ T Cell Differentiation during Viral Infection. *Immunity* **2007**, *27*, 393–405.
43. Sallusto, F.; Lanzavecchia, A.; Araki, K.; Ahmed, R. From Vaccines to Memory and Back. *Immunity* **2010**, *33*, 451–463.
44. Cui, W.; Kaech, S. M. Generation of Effector $CD8^+$ T Cells and Their Conversion to Memory T Cells. *Immunol. Rev.* **2010**, *236*, 151–166.
45. Demento, S. L.; Cui, W.; Criscione, J. M.; Stern, E.; Tulipan, J.; Kaech, S. M.; Fahmy, T. M. Role of Sustained Antigen Release from Nanoparticle Vaccines in Shaping the T Cell Memory Phenotype. *Biomaterials* **2012**, *33*, 4957–4964.
46. Zemser, M.; Friedman, M.; Katzhendler, J.; Greene, L. L.; Minsky, A.; Gorinstein, S. Relationship between Functional Properties and Structure of Ovalbumin. *J. Protein Chem.* **1994**, *13*, 261–274.
47. Torres, M. P.; Wilson-Welder, J. H.; Lopac, S. K.; Phanse, Y.; Carrillo-Conde, B.; Ramer-Tait, A. E.; Bellaire, B. H.; Wannemuehler, M. J.; Narasimhan, B. Polyanhydride Microparticles Enhance Dendritic Cell Antigen Presentation and Activation. *Acta Biomater.* **2011**, *7*, 2857–2864.